J. Plasma Physics (2010), *vol.* 76, *part* 1, *pp.* 29–37.
doi:10.1017/S0022377809008046

Effects of a non-monotonic safety factor on the particle transport and diffusion in the case of a reversed magnetic shear

M. GHABBOURI[1], D. SAIFAOUI[1], A. BOULEZHAR[1], A. DEZAIRI[2] and M. EL MOUDEN[1,3]

[1]Laboratory of Theoretical Physics, Faculty of Sciences Ain Chock, Casablanca, Morocco (s.ghabbouri@gmail.com)

[2]Laboratoire de Physique de la Matière Condensée, Faculté des Sciences Ben M'sik, B.P. 7955, Casablanca, Morocco

[3]Institut Jean Lamour, CNRS–Nancy-Université–UPV-Metz, UMR 7198, Département P2M, Université Henri-Poincaré, Nancy I, B.P. 239, 54506 Vandoeuvre les Nancy cedex, France

(Received 13 February 2009 and accepted 23 March 2009, first published online 30 April 2009)

Abstract. This work is based on a numerical study of particle transport and diffusion using ITER parameters. In particular, the effects of introducing a non-monotonic safety factor (NMSF) in the case of a reversed magnetic shear are shown. These results are compared with those found by using a monotonic safety factor (MSF). Double internal transport barriers are detected influencing the transport and diffusion of particles. The choices of the mode (m, n) and the m/n values play a dominant role for the particle diffusion, which leads to an improvement of the magnetic confinement.

1. Introduction

Among the improvements in plasma confinement performance observed in many worldwide tokamak devices since the 1990s [1,2], a reversed shear (RS) or negative central shear (NCS) regime is one of the most attractive concepts to prepare for the next-generation burning plasma experiments. Therefore, most present major tokamaks have been devoted to the study of this operation regime as an advanced tokamak (AT) operation. In this respect, the ITER is an international tokamak (magnetic confinement fusion) research proposal for an experimental project that will help to make the transition from today's studies of plasma physics to future electricity-producing fusion power plants. The RS regime is characterized by a negative or very low central magnetic shear region, and reduced thermal transport to near-neoclassical values and reduced particle transport have been observed in this regime. The reduction in the transport, caused by an internal transport barrier (ITB) formed in the core plasma of the tokamak, is related to the stabilization of micro-turbulences due to the sheared $E \times B$ flow and negative or very low magnetic shear [3]. Therefore, reproducing or predicting the ITB plasma through numerical simulations requires plasma transport models based on micro-turbulence-suppressing physics. In the present numerical work, we will focus on

the effects arising from the new profile of the security factor that allow us the more realistic scenario of particle transport and diffusion compared with [3–6]. Our paper is organized as follows. In Sec. 2, we present the equations of motion which describe the particle dynamics in a tokamak and their transformation into mapping equations, which are solved numerically. In Sec. 3, we present different numerical tests and compare with other works. We also compute the dependence of the diffusion coefficient on the values of (m, n), q_a and m/n. Finally, we end with a conclusion section.

2. Motion equations and mapping

2.1. Transport model and motion equations

The simplified model of an equilibrium magnetic field [3–7] is used and the magnetic field can be expressed as $\mathbf{B} = B_\theta \mathbf{e}_\theta + B_\varphi \mathbf{e}_\varphi$ according to the toroidal geometry, where $B_\theta = (r/qR_0)B_\varphi$ with r and q being respectively the plasma minor radius and the safety factor.

The equation of the guiding center in Gauss system units reads

$$\frac{d\mathbf{x}}{dt} = v_\parallel \frac{\mathbf{B}}{B} + c\frac{\mathbf{E}\otimes\mathbf{B}}{B^2}, \tag{1}$$

where $v_\parallel$ is the parallel velocity and the second term on the right of the equation represents the drift velocity. The electrostatic potential ϕ that satisfies the relation $\mathbf{E} = -\nabla\phi$ may be written as the sum of the radial part supposed at equilibrium and the fluctuating part $\phi = \phi_0 + \tilde{\phi}$. According to the model of the drift wave spectrum, $\tilde{\phi}$ takes the form $\sum_{mln} \phi_{mln} \cos(m\theta - l\varphi - nw_0 t)$ with w_0 being the lowest angular frequency in the spectrum. From $\tilde{\phi}$, we define the disrupted electric field $\tilde{E} = -\nabla\tilde{\phi}$, making the approximations $B_\theta \ll B_\varphi$ and $B_r = 0$. Equation (1) becomes like the system using toroidal coordinates:

$$\begin{aligned} \frac{dr}{dt} &= -\frac{c}{Br}\frac{\partial\tilde{\phi}}{\partial_\theta}, \\ r\frac{d\theta}{\partial t} &= v_\parallel \frac{B_\theta}{B} + \frac{c}{B}\frac{\partial\tilde{\phi}}{\partial r} - c\frac{\tilde{E}_r}{B}, \\ R\frac{d\varphi}{dt} &= v_\parallel. \end{aligned} \tag{2}$$

The first equation of (2) results when replacing $\tilde{\phi}$, and taking into account the following two properties of sine and cosine functions:

$$\sum_{n=-\infty}^{+\infty} \sin(nw_0 t) = 0, \quad \sum_{n=-\infty}^{+\infty} \cos(nw_0 t) = 2\pi\sum_n \delta(w_0 t - 2\pi n),$$

$$\frac{dr}{dt} = \frac{2\pi c}{Br}\sum_{mn} m\phi_{mn} \sin(m\theta - n\varphi)\delta(w_0 t - 2\pi n). \tag{3}$$

2.2. The mapping

In order to simplify the resolution of the system above, we use the mapping approach that consists of reducing the number of variables and equations. For this, we introduce the angle-action variables: $J = r^2/a^2$ and $\chi = m\theta - n\varphi$, where a is

https://doi.org/10.1017/S0022377809008046 Published online by Cambridge University Press

the small radius of the torus, and we consider only one mode of the perturbation (m, n); (3) then becomes

$$\frac{dJ}{dt} = \frac{2r}{a^2}\frac{dr}{dt} = \frac{4\pi c}{a^2 B} m\phi_{mn} \sin(m\theta - n\varphi) \sum_n \delta(w_0 t - 2\pi n), \tag{4}$$

$$\frac{d\chi}{dt} = m\frac{B_\theta}{r.B}\left(v_\parallel - c\frac{\bar{E}_r}{B_\theta}\right) - n\frac{v_\parallel}{R}. \tag{5}$$

We neglect the term $\bar{E}_r$. The integration of (4) and (5) with respect to the time t_n allows us to construct the mapping in its simple form:

$$J_{k+1} = J_k + \frac{4\pi c}{a^2.B_0}\frac{m\phi}{w_0}\sin(m\theta - n\varphi),$$

$$\chi_{k+1} = \chi_k + \frac{2\pi v_\parallel}{w_0 q.R}(m - nq). \tag{6}$$

In order to introduce the reversed magnetic shear and the radial electric field, we have used in our simulation the global mapping; in the following we give the algorithm

$$J_{k+1} = J_k + \frac{4\pi c}{a^2.B_0}\frac{m\phi}{w_0}\sin(m\theta_k - n\varphi_k),$$

$$\chi_{k+1} = \chi_k + RK1(J_{k+1}) + RK2(J_{k+1}),$$

with

$$RK1(J) = \frac{v_\parallel(J)}{2\pi w_0 qR}(m - nq(J)), \quad RK2(J) = -\frac{cm}{2\pi w_0 a B_0}\frac{\bar{E}_r(J)}{\sqrt{J}}$$

and

$$v_\parallel(J) = \sqrt{2(\xi_t - e.\phi_0(J))(1 - \lambda.B_0)/m};$$

here, ξ_t is the initial total energy, e is the particle charge, $\lambda = \mu/\xi_t$, where μ is the magnetic momentum, and ϕ_0 is the equilibrium potential that satisfies the relation $\bar{E}_r(J) = -(\partial\phi_0/\partial r)|_{r=a\sqrt{J}}$.

In our simulations, we focus only on the reversed magnetic shear with a non-monotonic safety factor (NMSF) that allows us to detect the formation of core transport barriers, for which substantial improved confinement can be concluded. The safety factor is expressed as

$$q(r) = q_a(r^2/a^2)[1 - (1 + \beta' r^2/a^2)(1 - r^2/a^2)^{\gamma+1}\theta(1 - r/a)]^{-1}, \tag{7}$$

with $q_a = I_\mathrm{p} a^2/I_\mathrm{e} R_0^2$ and $\beta' = \beta(\gamma + 1)/(\beta + \gamma + 2)$, where $I_\mathrm{p}, a, I_\mathrm{e}, R_0$ and β' are respectively the total plasma current, plasma radius, external current, the magnetic axis radius and the coefficient that describes the plasma current profile.

Our numerical tests are obtained using the ITER parameters with the following values: $a = 1.85$ m, $R_0 = 6.35$ m, the central magnetic field is taken as $B = 5.2$ T, $w_0 = 1.93 \times 10^5$, the disrupted modes are taken as $m = 12$, $n = 6$ and $\xi = 167$ eV; with this form of the equilibrium potential $\phi_0(r) = -\phi_0(1 - r^2/a^2)\exp(1 - r/a)$; because the function $\theta(1 - r/a)$ in (7) has no influence on the calculations, we have taken it as the unity function. The values of β', q_a and γ are, respectively, 0.93, 5 and 2.8. The numerical results are the particle trajectory structures in the plane $(\chi, r/a)$ found with the values of applied potential from 5 to 40 eV; these results are plotted with those of [3–6] in Fig. 1 in order to make a comparison easier.

https://doi.org/10.1017/S0022377809008046 Published online by Cambridge University Press

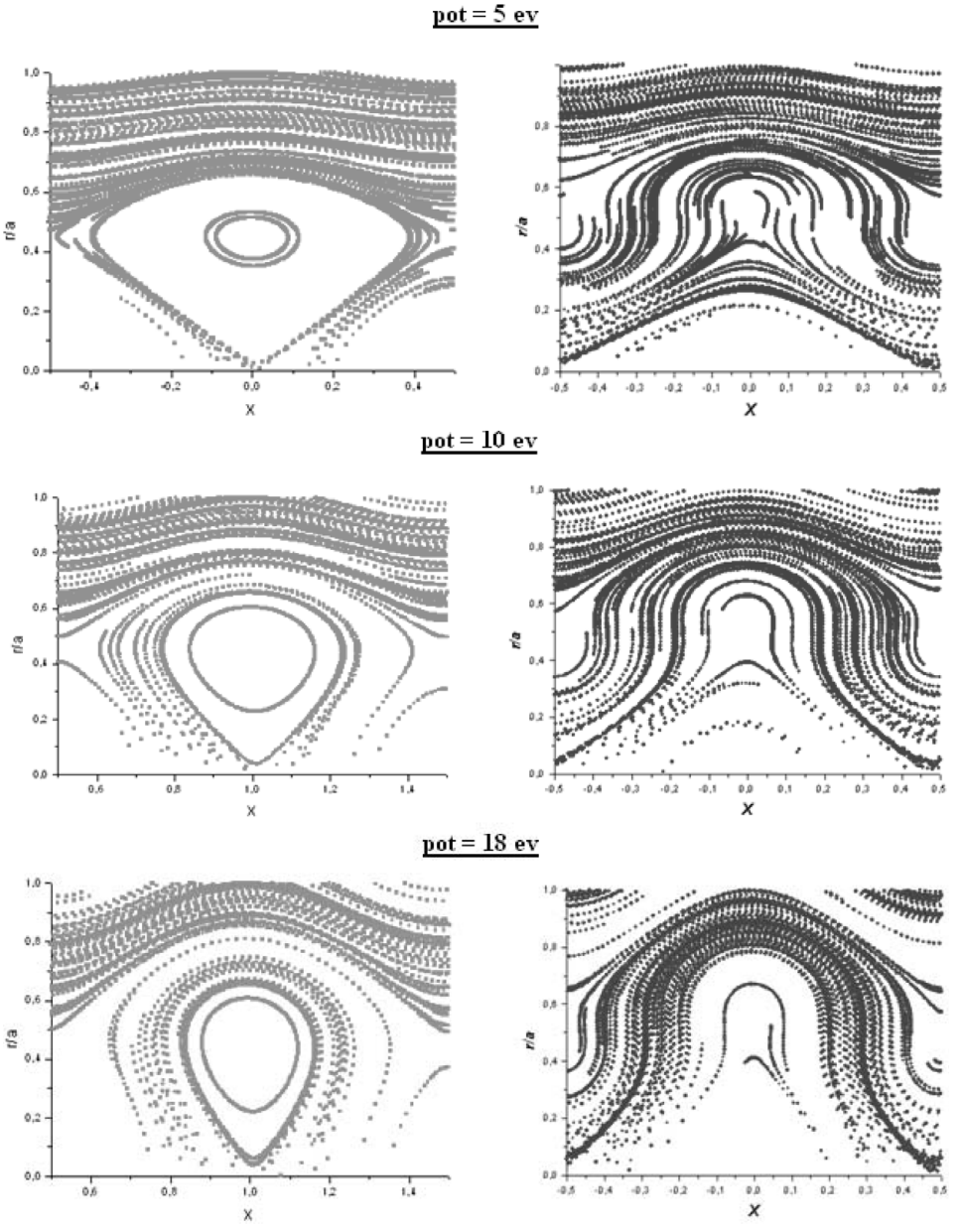

Figure 1. Poincaré section in the plane $(X, r/a)$ of 1000 particles with different values of potential. Figures on the left are plotted with a non-monotonic profile of the safety factor, those on the right with a monotonic profile.

3. The numerical results

3.1. Particle trajectory tests

The obtained numerical tests show the appearance of the so-called double internal transport barriers [8]. These are displaced toward the outer regions of the tokamak with increasing values of the applied potential; these kind of barriers play a

https://doi.org/10.1017/S0022377809008046 Published online by Cambridge University Press

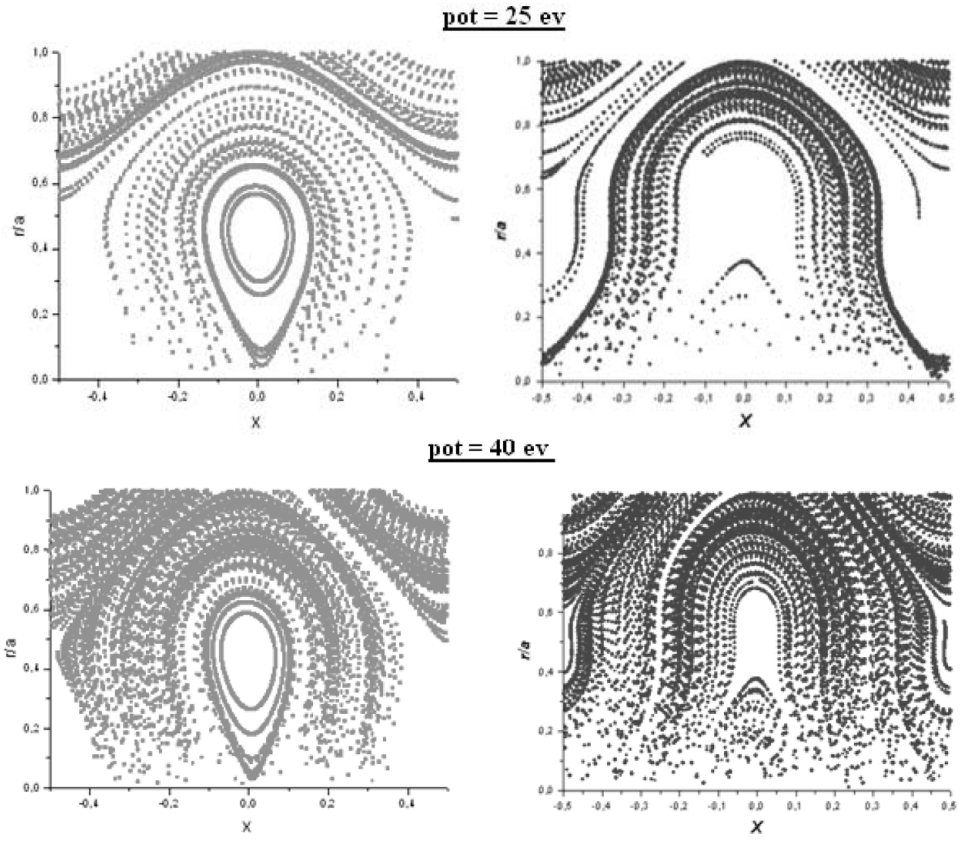

Figure 1. Continued.

potential role for decreasing the particle diffusion than the normal transport barriers calculated by using the reversed monotonic profile of the safety factor.

3.2. The particle diffusion tests

The particle diffusion coefficients are computed for different values of applied potential and compared to the ones of the monotonic profile of the safety factor [9, 10, 12]. Figure 2 shows the time evolution of the ratio of two diffusion coefficients calculated with the NMSF and the monotonic safety factor (MSF); for any value of applied potential the ratio $Dr_{\mathrm{rnmp}}/Dr_{\mathrm{rmp}}$ (rnmp: reversed-non monotonic profile; rmp: reversed monotonic profile) is always less than one. This means that in the case of NMSF the particle diffusion is less than the case of MSF, and this important result will contribute to improve the magnetic confinement.

3.3. The effects of (m, n), m/n and q_a on the particle diffusion

In this subsection, we will study numerically the effect of small, moderate and high perturbation mode values (m, n), their m/n values and the safety factor value at the plasma edge q_a on the diffusion coefficient. Figure 3 shows clearly the impact of the m/n value on the diffusion coefficient. In the first plot, the modes are chosen for which the m/n value is close to 2; the obtained result tells us that the diffusion decreases according to the perturbation mode values: for small values it takes the

https://doi.org/10.1017/S0022377809008046 Published online by Cambridge University Press

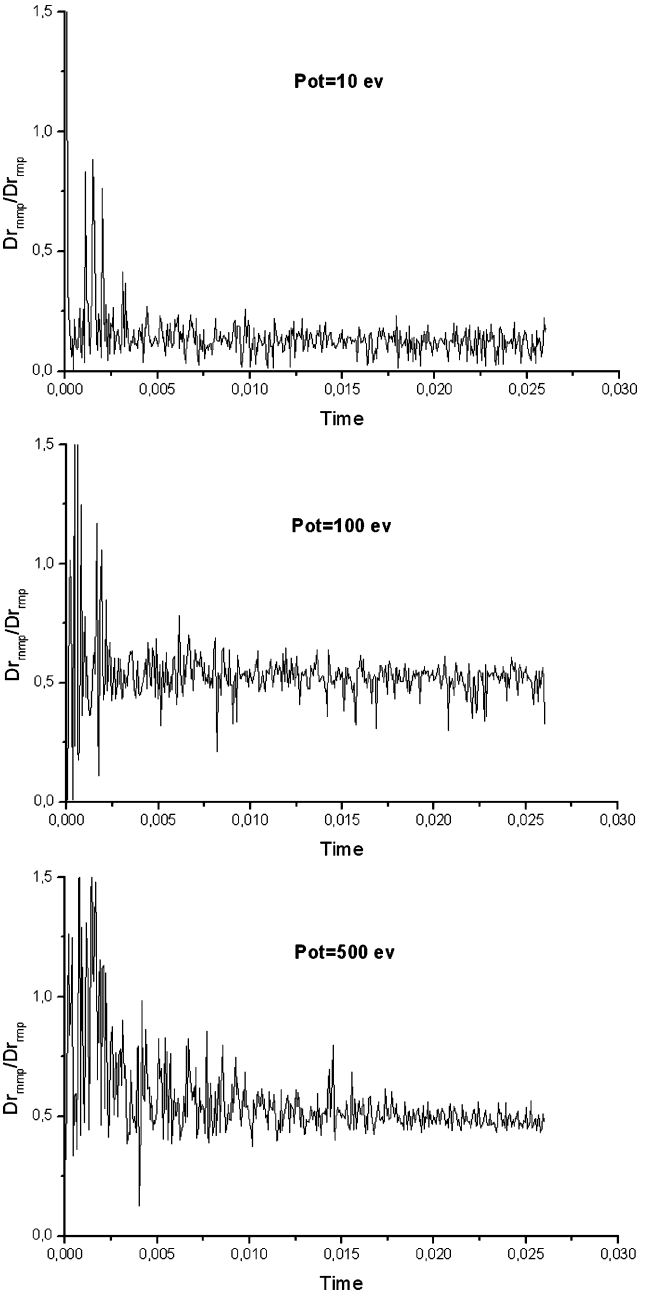

Figure 2. Time evolution of the ratio between reversed non-monotonic profile (rnmp) and reversed monotonic profile (rmp) of diffusion coefficients.

value 0.12, for moderate values it reaches 0.07 and, for the high modes of the perturbation, the diffusion coefficient decreases to the value 0.02. When $m/n = 4$, both the small and moderate modes of the perturbation lead to roughly the same values of the diffusion coefficient 0.12 and 0.11, and for the high mode the diffusion coefficient reaches the value 0.02. These tests inform us about the impact of the m/n

https://doi.org/10.1017/S0022377809008046 Published online by Cambridge University Press

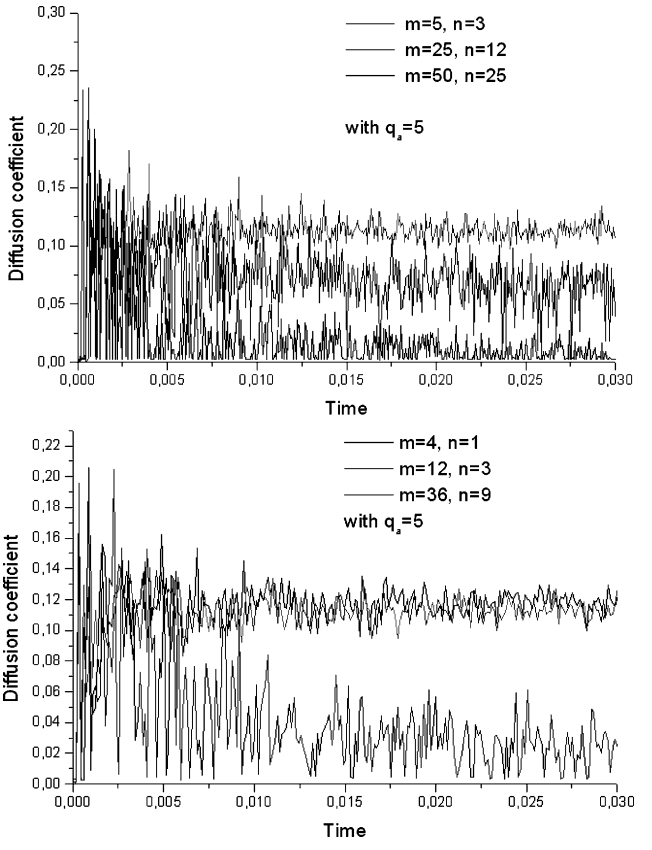

Figure 3. Diffusion coefficient with different values of the mode (m, n) of perturbation; the first plot corresponds to $m/n = 1.66$, 2.08 and 2. The second plot corresponds to $m/n = 4$, both plots are calculated with a fixed q_a (safety factor at the edge of the plasma).

value on the behavior of the particle diffusion; when this value is close to 2, there are the small, moderate and high modes to be studied; whereas when $m/n = 4$, we consider the fusion of small and moderate modes, since they lead to the same diffusion coefficient value, and the high mode that leads to the small value of the diffusion coefficient.

The plots in Fig. 3 are computed in order to confirm that there is no effect of taking high values of m/n (Fig. 4) and the variation of the q_a values on the diffusion of particles (Fig. 5), so what we can conclude from this simulation that the modes of the perturbation (m, n) and their m/n values (only those less than seven) play a fundamental role in the particle diffusion.

4. Conclusion

We have investigated the effects arising from introducing the NMSF in the case of reversed magnetic shear on the transport and the diffusion of particles. This investigation tell us that the profile used for the safety factor is more adequate compared to the MSF for ITER. We have plotted the trajectories of particles and computed the corresponding coefficients of diffusion; we have tested numerically

https://doi.org/10.1017/S0022377809008046 Published online by Cambridge University Press

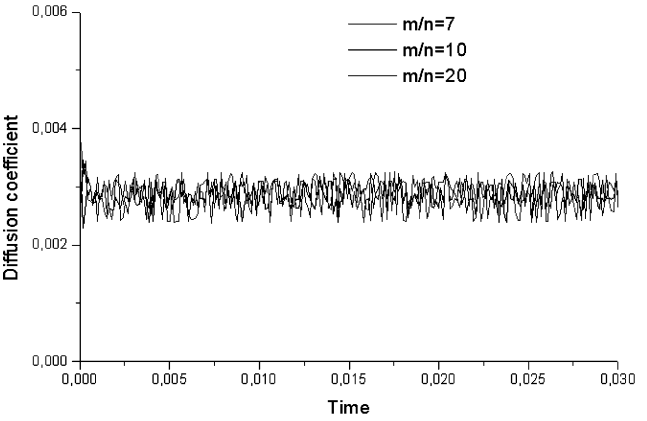

Figure 4. The diffusion coefficient behavior when the shift between m and n becomes important.

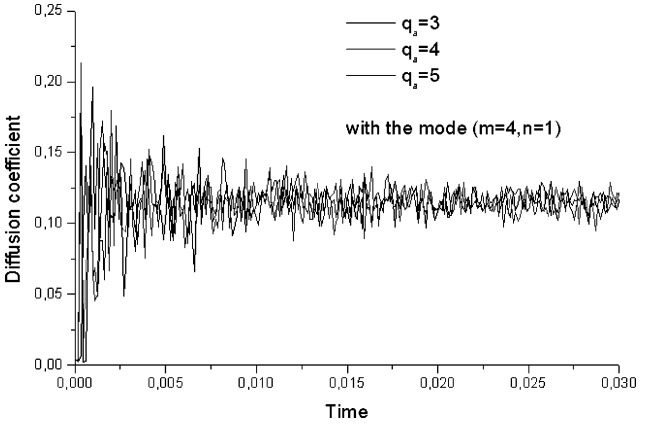

Figure 5. The particle diffusion coefficient calculated for different values of q_a, with a fixed mode of perturbation ($m = 4, n = 1$).

the effects of the mode (m, n), the parameter q_a and the m/n values on the diffusion of the particles. In future work we will study the chaotic diffusion caused by the magnetic chaotic field lines; for this we will use the superposition of a set of drift waves with a new potential form.

References

[1] Itoh, K., Itoh, S.-I. and Fukuyama, A. 1999 *Transport and Structural Formation in Plasmas*. Bristol: Institute of Physics of Publishing.

[2] Nagashima, Y. et al. 2006 *Plasma Phys. Control. Fusion* **48**, A377.

[3] El Mouden, M., Saifaoui, D., Dezairi, A., Zine, B. and Eddahbi, M. 2007 *J. Plasma Phys.* **73**(4), 439–453.

[4] El Mouden, M., Saifaoui, D., Dezairi, A. and Imzi, H. 2005 Use of magnetic shear for the improvement of quality of confinement in the plasma of tokamak. *FIZIKA A* **14**(4), 277–288.

https://doi.org/10.1017/S0022377809008046 Published online by Cambridge University Press

[5] El Mouden, M., Saifaoui, D., Dezairi, A. and Imzi, H. 2004 *Moroccan J. Condens. Matter* **5**(2), 202–208.

[6] El Mouden, M., Saifaoui, D., Dezairi, A., Zine, B., Eddahbi, M. and Rouak, A. 2007 The influence of magnetic reversed shear in the improvement of quality of confinement in the plasma of tokamak: comparison between TEXTOR & ITER. *Moroccan J. Condens. Matter* **9**(1), 20–27.

[7] Tabet, R., Saifaoui, D., Dezairi, A. and Rouak, A. 1998 *Eur. Phys. J. AP* **4**, 329.

[8] Marcus, F. A., Kroetz, T., Roberto, M., Caldas, I. L., Da Silva, E. C., Viana, R. L. and Guimaraes-Filho, Z. O. 2008 Chaotic transport in reversed shear tokamaks. *Nucl. Fusion* **48**, 024018–024026.

[9] Kamada, Y. 2000 Observations on the formation of transport barriers. *Plasma Phys. Control. Fusion* **42**, A65–A80.

[10] Antoni, V. et al. 2000 Electrostatic transportation reduction induced by flow shear modification in a reversed field pinch plasma. *Plasma Phys. Control. Fusion* **42**, A271–A276.

[11] Oualyoudine, A., Saifaoui, D., Dezairi, A. and Rouak, A. 1997 *J. Physique* **7**, 1045.

[12] Takenaga, H. et al. 1998 Determination of particle transport coefficients in reversed shear plasma of JT-60U. *Plasma Phys. Control. Fusion* **40**, 183–190.